# Glut1-mediated glucose transport regulates HIV infection

Séverine Loisel-Meyer[a,1], Louise Swainson[a,1,2], Marco Craveiro[a,b], Leal Oburoglu[a], Cédric Mongellaz[a], Caroline Costa[c], Marion Martinez[a], François-Loic Cosset[c], Jean-Luc Battini[a], Leonard A. Herzenberg[d,3], Leonore A. Herzenberg[d], Kondala R. Atkuri[d], Marc Sitbon[a], Sandrina Kinet[a], Els Verhoeyen[c], and Naomi Taylor[a,3]

[a]Institut de Génétique Moléculaire de Montpellier, Centre National de la Recherche Scientifique, Unité Mixte de Recherche 5535, F-34293 Montpellier Cedex 5, France; [b]Center for Neurosciences and Cell Biology, University of Coimbra, 3030-790 Coimbra, Portugal; [c]Ecole Normale Supérieure de Lyon, Institut National de la Santé et de la Recherche Médicale, Unité Mixte de Recherche 758, F-69364 Lyon Cedex 7, France; and [d]Department of Genetics, Stanford University School of Medicine, Stanford, CA 94305

Cell cycle entry is commonly considered to positively regulate HIV-1 infection of CD4 T cells, raising the question as to how quiescent lymphocytes, representing a large portion of the viral reservoir, are infected in vivo. Factors such as the homeostatic cytokine IL-7 have been shown to render quiescent T cells permissive to HIV-1 infection, presumably by transiently stimulating their entry into the cell cycle. However, we show here that at physiological oxygen (O$_2$) levels (2–5% O$_2$ tension in lymphoid organs), IL-7 stimulation generates an environment permissive to HIV-1 infection, despite a significantly attenuated level of cell cycle entry. We identify the IL-7–induced increase in Glut1 expression, resulting in augmented glucose uptake, as a key factor in rendering these T lymphocytes susceptible to HIV-1 infection. HIV-1 infection of human T cells is abrogated either by impairment of Glut1 signal transduction or by siRNA-mediated Glut1 down-regulation. Consistent with this, we show that the susceptibility of human thymocyte subsets to HIV-1 infection correlates with Glut1 expression; single-round infection is markedly higher in the Glut1-expressing double-positive thymocyte population than in any of the Glut1-negative subsets. Thus, our studies reveal the Glut1-mediated metabolic pathway as a critical regulator of HIV-1 infection in human CD4 T cells and thymocytes.

thymus | metabolism | hypoxia

T he productive infection of both naive and memory CD4 T cells by HIV-1, at least outside the context of lymphoid tissues (1, 2), requires a transition into the G1b stage of the cell cycle (3). As most circulating peripheral T lymphocytes are in the G0 resting state, this would theoretically preclude their infection by HIV-1. However, within lymphoid aggregates, HIV-1 infection can occur in quiescent naive T cells (1, 2), although this phenomenon has recently been shown to be associated with the expression of activation markers (4, 5). Under what conditions can HIV-1 infection be achieved in quiescent T lymphocytes that remain phenotypically naive? One possibility is that the in vivo infection of naive CD4$^+$ T cells occurs following exposure of these lymphocytes to cytokines such as IL-7. Indeed, IL-7 stimulation is currently thought to be critical for activating the latent HIV reservoir (6–8). Thus, the infection status of quiescent T cells under physiological conditions, either in the absence or presence of IL-7, remains to be addressed.

IL-7 is a 25-kDa glycoprotein produced in thymus, intestine, skin, lymph nodes, and other sites (reviewed in ref. 9). It plays a major role in the in vivo maintenance of polyclonal naive and memory T cells, positively regulating the survival, differentiation, and proliferation of thymocyte and peripheral T-lymphocyte populations. The homeostatic maintenance of this polyclonal T-cell pool is required for the persistence of immunologic memory as well as for the maintenance of naive T cells with the potential to respond to novel antigens. Under conditions of lymphopenia, IL-7 supports a transient homeostatic T-cell proliferation, promoting the expansion of T cells with a diverse T-cell receptor (TCR) repertoire. However, under physiological conditions, the vast majority of peripheral lymphocytes are quiescent, perhaps because

homeostatic levels of IL-7 are low relative to peripheral T-cell numbers (reviewed in ref. 10). Indeed, serum IL-7 levels are increased in patients with lymphopenia, secondary to either HIV-1 infection or chemotherapy (reviewed in ref. 10). Consistent with these findings, administration of exogenous IL-7 in preclinical murine and primate studies has been shown to promote T-cell survival and proliferation with short-term expansion of de novo generated recent thymic emigrants (reviewed in ref. 10). Moreover, in recent clinical trials, the administration of recombinant IL-7 led to a transient entry of T lymphocytes into the cycle, albeit with a rapid return to quiescence (11–15).

To date, studies of IL-7 stimulation and IL-7 signaling intermediates ex vivo have been performed almost exclusively in incubators maintained at atmospheric O$_2$ levels (20% O$_2$). However, tissue O$_2$ levels in vivo are substantially lower: direct in vivo measurements of O$_2$ levels in murine lymphoid organs have revealed partial pressures of 0.5–4.5% (16), somewhat higher O$_2$ levels in peripheral blood, and 14% in alveoli (17, 18). Thus, although lymphocytes encounter fluctuations in O$_2$ levels in vivo, the physiological range of O$_2$ levels to which they are exposed is at least two to six times lower than the 20% O$_2$ levels maintained in standard incubators. Culturing at atmospheric O$_2$ levels has been shown to result in altered cell proliferation rates and other skewed T-cell responses (16, 19–23). Thus, because the goal of in vitro studies is generally to reveal information of in vivo significance, our studies here focus on findings with peripheral blood T cells cultured at physiological O$_2$ levels. Here we assessed how naive and memory T cells respond to IL-7 at the O$_2$ levels to which they are exposed in vivo and determined their susceptibility to HIV-1 infection.

## Results

**Physiological O$_2$ Levels Decrease IL-7–Induced Cell Cycle Entry Without Modulating Proximal IL-7 Signaling.** IL-7 has long been known to be a survival factor for T lymphocytes both ex vivo and in vivo. Nevertheless, the effects of IL-7 on T lymphocytes cultured under physiological O$_2$ concentrations have not been evaluated. IL-7 stimulation of freshly isolated CD4 T lymphocytes promoted a high level of viability, irrespective of whether the cells were cultured at 20% (atmospheric) or 2.5% (physiological) O$_2$ concentrations (Fig. S1). Both forward scatter (FSC), a measure of cell size, and

side scatter (SSC), a function of cell granularity, profiles of the cells were increased by IL-7 stimulation, but the increase was significantly higher under atmospheric compared with physiological $O_2$ conditions. Specifically, in both naive and memory CD4 T cells, FSC and SSC were increased by ∼20% and 50–60%, respectively, following IL-7 stimulation at atmospheric $O_2$, whereas these parameters were only increased by 5% and 20% at physiological $O_2$ (Fig. S1; $P < 0.05$ for both naive and memory T cells; $n = 3$). Differences in these physical parameters were the first indication that $O_2$ concentration impacts on IL-7–mediated effects.

Indeed, IL-7–induced cell cycle entry, monitored as a function of DNA/RNA levels, was significantly lower under conditions of 2.5% $O_2$ for both naive and memory CD4 T cells ($P < 0.0001$ and $P < 0.01$, respectively, at day 9; $n = 4$; Fig. 1A and Fig. S2). Indeed, the percentages of IL-7–stimulated naive or memory CD4 T cells entering into S/G2/M at day 9 were 10-fold lower under physiological compared with atmospheric $O_2$, and this phenomenon was observed throughout the 12 d of IL-7 stimulation (Fig. S2). Furthermore, this difference was not restricted to the DNA replication phase of the cell cycle, as levels of Ki67, expression of which is acquired as early as mid-G1, were also significantly lower following IL-7 stimulation of naive and memory CD4 T cells at physiological compared with atmospheric $O_2$ concentrations ($P < 0.05$ for both subsets at day 9; $n = 3$; Fig. S2).

Given the significant differences in IL-7–mediated cell cycle entry under 20% and 2.5% concentrations, it was important to determine whether IL-7 was able to efficiently induce proximal signaling pathways under the latter conditions. Interaction of IL-7 with its receptor is known to result in receptor internalization and decreased receptor transcription, resulting in a decrease in surface IL-7Rα levels (24–26). We indeed observed IL-7Rα down-regulation on naive as well as memory CD4 T cells, irrespective of the $O_2$ concentration at which the lymphocytes were cultured (Fig. 1B). Moreover, IL-7 stimulation resulted in a similar phosphorylation of STAT5 at 20% and 2.5% $O_2$ concentrations [nonsignificant (NS), $P > 0.05$; $n = 5$]. STAT5 phosphorylation was detected under both conditions between days 1 and 6 following IL-7 stimulation (Fig. 1C), strongly suggesting that proximal IL-7 signaling was not inhibited by the $O_2$ concentration at which the T cells were cultured. However, upon assessment of a late activation marker, the CD71 transferrin receptor, significant induction was detected only upon IL-7 stimulation of naive and memory CD4 T cells at atmospheric $O_2$ and only at late time points (Fig. 1D and Fig. S3). Thus, IL-7 signaling is induced under both atmospheric and physiological $O_2$ conditions, but transmission of this signal, as assessed by CD71 up-regulation and cell cycle entry, is dependent on the $O_2$ concentration to which the T cells are exposed.
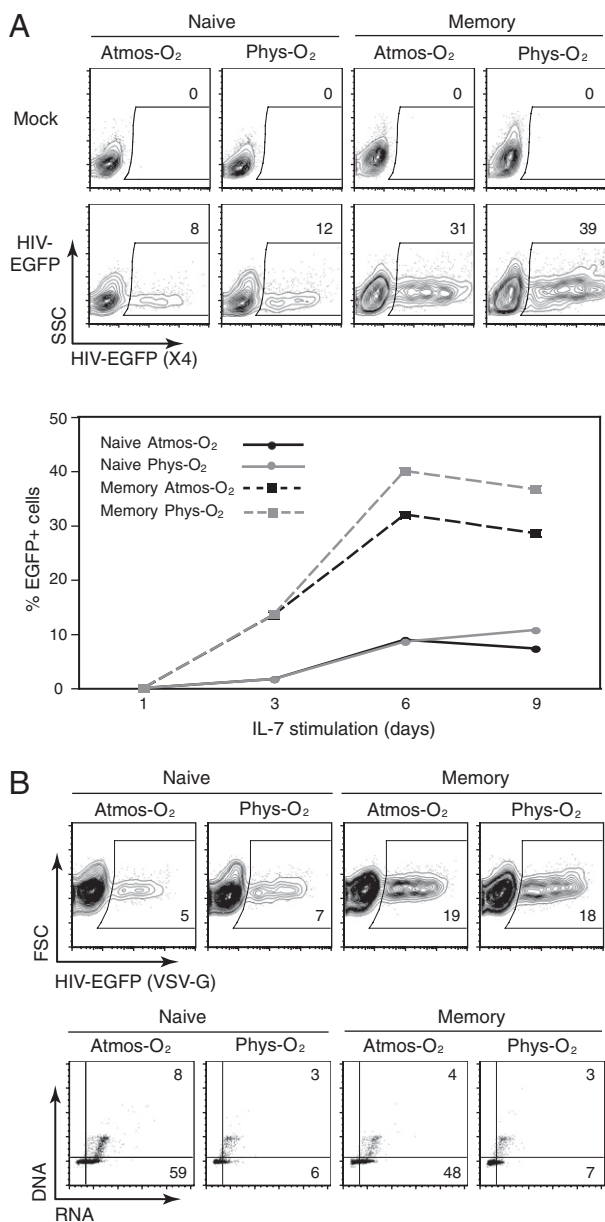
**Susceptibility of IL-7–Stimulated CD4 T Cells to Single-Round HIV-1 Infection Is Maintained Under Physiological $O_2$ Concentrations.** HIV-1 infection of CD4 T cells is known to be highly dependent on T cell activation and cell cycle entry and, indeed, the permissivity of quiescent lymphocytes to HIV-1 infection is extremely inefficient (reviewed in ref. 5). As we found that expression of activation markers and cell cycle entry were markedly inhibited at 2.5% $O_2$ (Fig. 1), we postulated that HIV-1 infection would be reduced at 2.5% $O_2$ relative to 20% atmospheric $O_2$ levels. To address this issue, we performed single-round infections of IL-7–stimulated T lymphocytes with X4-HIV-1 virions harboring the *eGFP* transgene. Interestingly, equivalent infection levels were observed at physiological and atmospheric $O_2$ (NS, $P > 0.05$ for both naive and memory T cells; $n = 3$). However, memory CD4 T cells were always infected at significantly higher levels than their naive counterpart (∼30% and 10% at day 6, respectively, in the representative donor shown; Fig. 2A).

Given this result, it was critical to determine whether the unexpectedly high levels of infection at 2.5% $O_2$ were due to changes in coreceptor expression. IL-7 has previously been shown to augment CXCR4 levels (27), and we found this to be the case in both naive and memory T cells. At physiological $O_2$ concentrations, CXCR4 levels were modestly increased by a further 16% in the memory subset ($P = 0.03$; $n = 8$). In naive
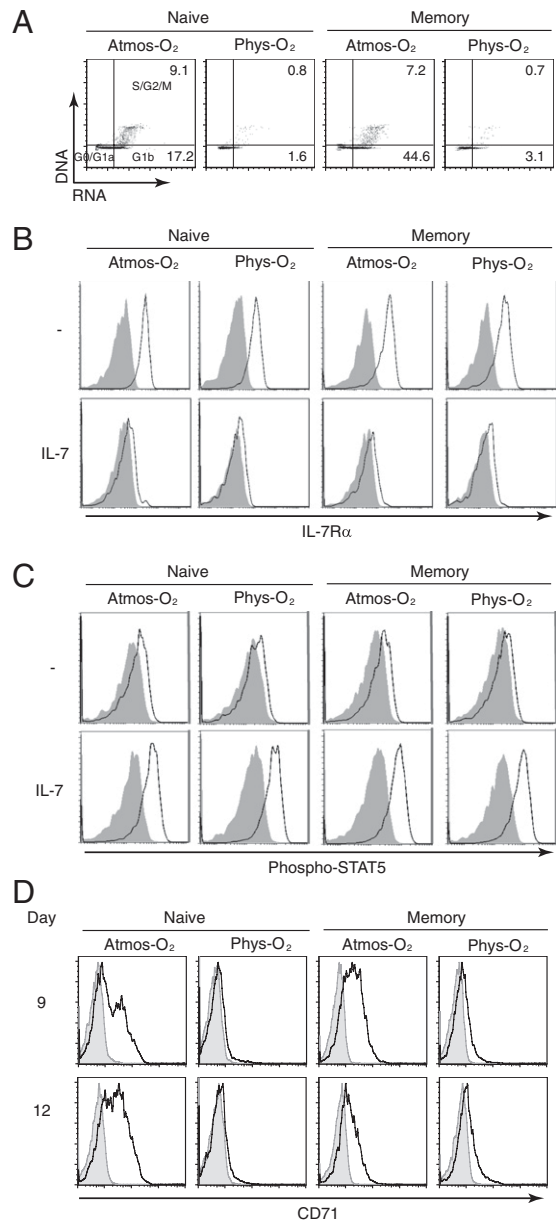


**Fig. 1.** Physiological $O_2$ levels diminish IL-7–induced cell cycle entry while maintaining proximal IL-7Rα signaling. Naive and memory CD4 T cell populations isolated from adult peripheral blood (APB) were stimulated with IL-7 (10 ng/mL) under 20% (Atmos-$O_2$) or 2.5% (Phys-$O_2$) $O_2$ conditions. (A) Cell cycle entry was monitored as a function of DNA and RNA levels, using 7-amino-actinomycin-D (7AAD) and pyronin Y (PY), respectively. PY/7AAD cell cycle staining is shown at day 9, and the percentages of cells in the G1b (lower right quadrant) and S/G2/M stages (upper right quadrant) are indicated. Cells in the lower left quadrant are in G0/G1a. (B) Expression of CD127, the IL-7Rα chain, was monitored at day 3, and specific staining (open histograms) compared with control isotype (closed histograms) is shown. (C) STAT5 phosphorylation was measured using an anti–phospho-STAT5 polyclonal antibody. Specific (open histograms) relative to control isotype staining (closed histograms) is shown in the presence or absence of IL-7. (D) CD71 transferrin receptor expression (open histograms) and isotype controls (closed histograms) were monitored at days 9 and 12 of IL-7 stimulation. Data are representative of three independent experiments comprising three to six different donors.

CD4 T cells, CXCR4 levels were comparable, irrespective of $O_2$ concentration (NS, $P > 0.05$; $n = 8$; Fig. S4), making it unlikely that the infection detected at physiological $O_2$ levels resulted from changes in coreceptor levels.

Loisel-Meyer et al.

**Fig. 2.** Permissivity of IL-7–stimulated CD4 T lymphocytes to infection by X4- and VSV-G–pseudotyped HIV-1 virions does not correlate with cell cycle kinetics under physiological $O_2$ concentrations. (*A*) Naive and memory CD4 T cell populations isolated from APB were stimulated for 1, 3, 6, or 9 d with IL-7 (10 ng/mL) under 20% (Atmos-$O_2$) or 2.5% (Phys-$O_2$) conditions and then infected with an X4-tropic HIV-1 vector harboring the EGFP reporter gene. Single-round infected cells were detected by monitoring EGFP expression 48 h postinfection. Representative dot plots are shown for infections performed at day 9 of IL-7 stimulation, and the percentages of infected EGFP+ cells are indicated (*Upper*). The *Lower* panel shows a quantification of the percentages of EGFP+ cells from infections performed at the indicated time points. (*B*) Nine days post–IL-7 stimulation, naive and memory CD4 T cells were infected with a VSV-G envelope-pseudotyped HIV-1 vector expressing EGFP. The percentages of EGFP+ cells are indicated (*Upper*). The corresponding level of cell cycle entry, assessed at the time of infection by PY/7AAD staining, is shown (*Lower*). The percentages of cells in the G1b (lower right quadrant) and S/G2/M (upper right quadrant) phases of the cell cycle are indicated (*Lower*). Data are representative of three independent experiments comprising three to eight different donors.

To exclude the possibility that the surprisingly high infection at physiological $O_2$ was due to enhanced gp120–CXCR4 interactions, we assessed single-round infection using HIV-1–based virions pseudotyped with the VSV-G envelope glycoprotein. The receptor

for this envelope glycoprotein appears to be ubiquitously expressed on all mammalian cells. As shown in Fig. 2*B*, infection by VSV-G–pseudotyped HIV-1 virions was not decreased at 2.5% $O_2$ (NS, $P > 0.05$ for both naive and memory T cells; $n = 8$). Notably, though, memory CD4 T cells remained significantly more susceptible to infection than naive T cells, irrespective of the $O_2$ concentration (18–19% compared with 5–7% infection, respectively; Fig. 2*B*). Thus, neither X4- nor VSV-G–mediated HIV-1 infection is decreased at physiological $O_2$ concentrations despite a highly reduced level of activation and cell cycle entry (Fig. 2*B*).

Recent thymic emigrants (RTE) show increased proliferation to IL-7 compared with long-term resident peripheral T cells (28–30). It was therefore of interest to determine whether IL-7 stimulation of RTE under physiological $O_2$ concentrations would also result in a diminished cell cycle entry and how this would impact on the permissivity of these cells to HIV-1 infection. RTE, characterized by a naive immature phenotype, represents the vast majority of T cells present in neonates and umbilical cord blood (UCB). IL-7 stimulation of UCB CD4 T cells at 2.5% $O_2$ resulted in a significantly attenuated level of cell cycle entry ($P < 0.05$; $n = 3$), with an effect similar to that which we observed in mature peripheral blood CD4 T cells (Fig. S5). Moreover, like mature CD4 T cells, the infection of IL-7–stimulated UCB CD4 T cells was not attenuated at 2.5% $O_2$ (NS, $P > 0.05$; $n = 5$; Fig. S5), providing further evidence that decreased cell cycle entry did not modulate infection of IL-7–stimulated CD4 T cells at physiological $O_2$ concentrations.
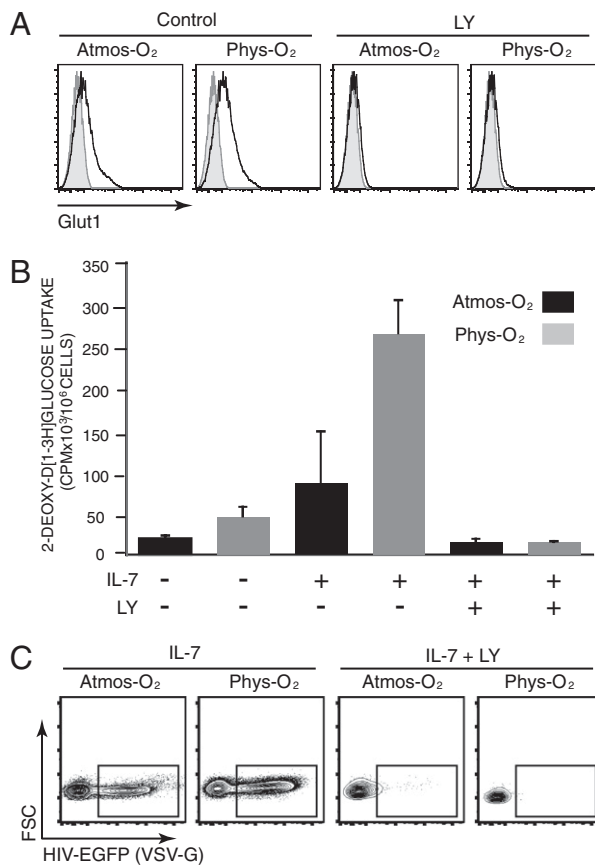
**Stimulation of CD4 T Cells at Physiological $O_2$ Concentrations Results in Enhanced Surface Glut1 Expression and Glucose Uptake.** It has long been postulated that the inability of quiescent T cells to be efficiently infected by HIV-1 is likely due, at least in part, to their very low metabolic state. Whereas this characteristic was once thought to be the default mode of T lymphocytes, it is now known that many factors actively control this quiescence (reviewed in ref. 5). One intriguing possibility to explain the permissivity of IL-7–stimulated T cells to HIV infection at low $O_2$ concentrations, even in the absence of cell cycle entry, is an enhanced metabolic activity and, specifically, an augmented uptake and utilization of glucose. This hypothesis is based, at least in part, on previous data showing that expression of the ubiquitous glucose transporter Glut1 is up-regulated in response to low $O_2$ in several cell types (31). Although Glut1 has not been detected at significant levels at the surface of quiescent T cells (32–34), it is induced by TCR stimulation (35, 36), as well as by the IL-7 cytokine (34, 37, 38).

Surface Glut1 expression was significantly augmented following IL-7 stimulation at 2.5% $O_2$ conditions compared with 20% $O_2$ (Fig. 3*A*; $P < 0.05$; $n = 8$). Furthermore, this increase in surface Glut1 expression was accompanied by a 300% increase in glucose uptake at physiological $O_2$ concentrations, as measured by the ability to uptake nonhydrolyzable 2-deoxy-D-[1-$^3$H]glucose (Fig. 3*B*).

**HIV-1 Infection Is Abrogated in the Absence of Surface Glut1.** Glut1 is a downstream substrate of the AKT/PI3K pathway, as assessed in both lymphocyte and nonlymphocyte lineage cells (reviewed in refs. 39 and 40). Moreover, expression of an activated transgenic Akt in murine T cells was found to result in an augmented glycolysis (32). To determine the role of this pathway in IL-7–induced surface Glut1 induction and subsequent HIV-1 infection, we used a PI3K inhibitor, LY294002. Incubation of IL-7–stimulated T cells with the LY294002 inhibitor resulted in an almost complete suppression of surface Glut1 as well as glucose uptake, both under 20% and 2.5% $O_2$ conditions (Fig. 3 *A* and *B*). This LY294002-mediated Glut1 inhibition was sufficient to completely abrogate single-round HIV-1 infection under either $O_2$ condition (Fig. 3*C*).
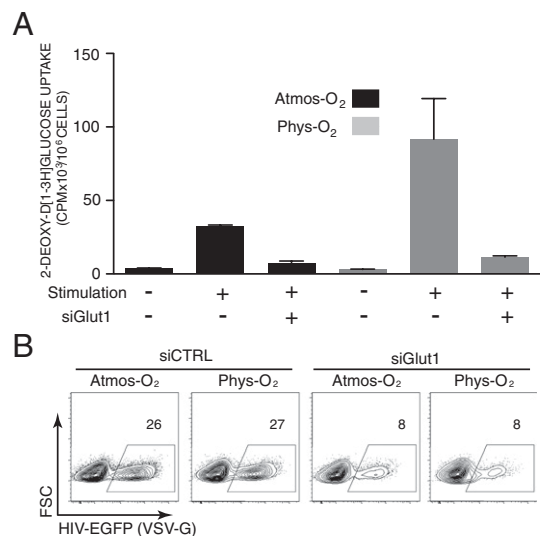
To verify that this effect was mediated by the Glut1 transporter itself, we used siRNAs directed against the Glut1 3′ UTR to specifically down-modulate endogenous Glut1 expression (41). Transfection of a mix of three different Glut1 siRNAs led to an approximate 70% decrease in Glut1 mRNA, to levels similar to those detected in nonstimulated CD4 T cells (Fig. S6).

MEDICAL SCIENCES

**Fig. 3.** IL-7–induced expression and function of the Glut1 glucose transporter are enhanced under physiological $O_2$ conditions, and its PI3K-mediated abrogation results in attenuated HIV-1 infection. (*A*) IL-7–stimulated APB CD4 T cells were cultured in the absence or presence of the PI3K inhibitor LY294002 (LY; 15 μM) and, at day 3, Glut1 expression was monitored. Representative histograms show specific Glut1 staining (open) relative to control staining (filled). (*B*) Glucose uptake was monitored in $1 \times 10^6$ CD4 T cells cultured for 3 d in the absence (–) or presence (+) of IL-7 and the LY inhibitor, as above. Lymphocytes were incubated with 2-deoxy-D-[1-$^3$H]glucose (2 μCi) for 10 min at room temperature. Results are expressed as mean cpm ± SD for triplicate sample analysis from cells cultured under 20% (black) or 2.5% (gray) $O_2$ conditions. (*C*) IL-7–stimulated CD4 T cells, cultured in the absence or presence of LY, were infected with VSV-G–pseudotyped HIV-EGFP virions. Infection was monitored 48 h later and the percentages of EGFP$^+$ cells are indicated. Data are representative of results obtained in six independent experiments comprising seven different donors.



**Fig. 4.** Inhibition of Glut1 up-regulation attenuates HIV-1 infection under atmospheric and physiological $O_2$ conditions. (*A*) CD4 T cells from APB were transfected with Glut1-specific siRNAs (siGlut1) and then stimulated under 20% (Atmos-$O_2$) or 2.5% (Phys-$O_2$) conditions for 24 h. Glucose uptake was monitored by incubating cells with 2-deoxy-D-[1-$^3$H]glucose (2 μCi) for 10 min at room temperature. Results are expressed as mean cpm ± SD for triplicate samples. (*B*) CD4 T cells stimulated following transfection with control (siCTRL) or Glut1-specific siRNAs were infected with VSV-G–pseudotyped HIV-EGFP virions. Infection was monitored at 48 h and the percentages of EGFP$^+$ cells are indicated. Data are representative of results obtained in four independent experiments comprising four different donors.

Moreover, this decrease in Glut1 mRNA resulted in a 70–80% attenuation in glucose uptake under both physiological and atmospheric $O_2$ conditions (Fig. 4*A*). The decrease in Glut1 and glucose uptake resulted in an average 70% inhibition of HIV-1 infection under both atmospheric and physiological $O_2$ conditions (Fig. 4*B*). Thus, the susceptibility of CD4 T cells to HIV-1 infection, at both physiological and atmospheric $O_2$ conditions, is regulated via the activity of the Glut1 glucose transporter.

**Glut1-Expressing Human Double Positive (DP) Thymocytes Present a Significantly Enhanced Susceptibility to HIV-1 Infection.** Thymocyte destruction by X4-tropic HIV-1 initially occurs in the DP population (42), and preferentially in those DP cells expressing higher levels of CD4 (CD4hiDP) and CXCR4 (43). Intriguingly, we previously found that Glut1 is expressed on ~10% of all human thymocytes, and this marker characterizes a subset of DP cells with high CD4 expression (44). As shown in Fig. 5*A*, CD4hiDP thymocytes express significantly higher levels of Glut1 and CXCR4 than CD4loDP thymocytes or single-positive (SP) SP8 or SP4 thymocytes. On the basis of the data obtained in CD4

T cells, it was possible that the high metabolic activity of CD4hiDP thymocytes conditioned their susceptibility to HIV-1 infection. We hypothesized that high surface Glut1 expression may result in an augmented susceptibility of these cells to HIV-1 infection, notwithstanding their high CD4 and CXCR4 receptor levels.

To test this hypothesis, we needed to infect thymocytes in a manner that bypassed the CD4/CXCR4 entry requirement. As such, we infected thymocytes with HIV-1 virions pseudotyped with the pantropic VSV-G envelope and, to avoid bias resulting from thymocyte mortality, freshly isolated total thymocytes were infected for only 12 h. At that time, thymocyte populations were sorted and immediately lysed for DNA extraction. Nested PCR was performed to analyze viral reverse-transcription products (GFP) and integrated provirus (Alu-LTR products). Notably, the HIV-1 core virions infected Glut1+DP thymocytes with significantly higher efficacy than other thymocyte populations. Enhanced infection was largely generated at a stage in the viral life cycle that occurred before or during reverse transcription, with a 6.5-fold higher level of GFP DNA in CD4hiDP compared with CD4loDP thymocytes. Levels of nuclear entry and integration were correspondingly higher, with seven- to ninefold increases in integrated Alu-LTR products in this subset compared with either Glut1-CD4loDP or SP subsets (Fig. 5*B*). The preferential infection of the CD4hiDP population could potentially promote the transmission of HIV-1 to more mature thymocyte progeny, resulting in a reservoir of infected T lymphocytes in vivo (43). This finding has important implications for the subsequent maintenance of the virus in a quiescent T-cell pool.

## Discussion

Here we show that IL-7–mediated activation and cell cycle entry are strikingly altered by the $O_2$ concentration to which CD4 T cells are exposed. Notably, though, IL-7 stimulation renders CD4 T lymphocytes susceptible to HIV-1 infection, irrespective of the $O_2$ concentration. We find that it is Glut1-mediated glucose uptake, rather than cell cycle entry per se, that regulates HIV-1 infection in
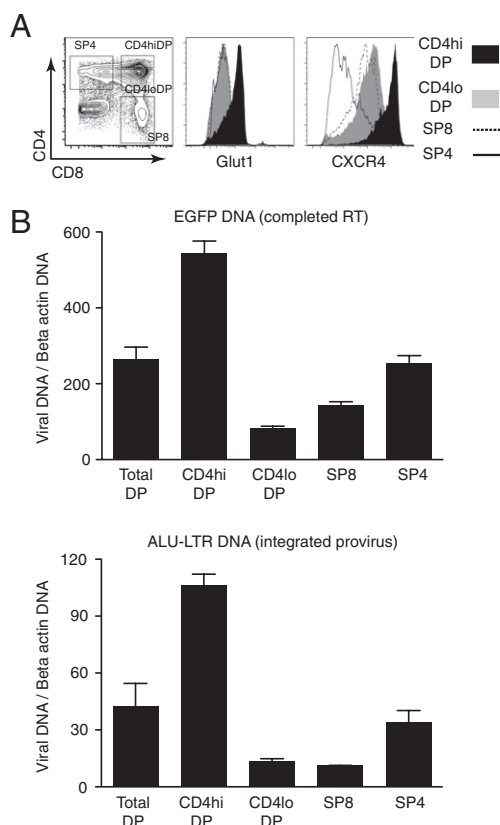
**Fig. 5.** Glut1 expression is associated with increased permissivity of the CD4hiCXCR4hi DP human thymocyte subset to VSV-G–pseudotyped HIV-1 infection. (A) Glut1 and CXCR4 staining in the CD4hiDP, CD4loDP, SP4, and SP8 human thymocyte subsets are shown as histogram overlays. The gates used to define and FACS sort these subsets are shown, and the percentages of cells in each quadrant are indicated. (B) Freshly isolated human thymocytes were infected for 12 h with a single-round VSV-G–pseudotyped HIV-1. Thymocyte populations were subsequently sorted by FACS and quantitative PCR analysis was performed to detect EGFP DNA (Upper), indicative of completed reverse transcription, as well as a two-step nested PCR for Alu-LTR DNA to detect integrated provirus (Lower). Signals were normalized to β-actin DNA. Results for each subset are expressed as means ± SD of triplicate samples.

these cells, establishing a unique paradigm for HIV-1 infection. Permissivity to HIV-1 infection was directly dependent on Glut1 activity, as Glut1-specific siRNAs inhibited infection of both X4- and VSV-G–pseudotyped viruses. Furthermore, within the human thymus, where Glut1 is differentially expressed, HIV-1 infection was markedly higher in the Glut1-expressing DP subset compared with Glut1-negative thymocytes. Therefore, we identify the Glut1-mediated metabolic pathway as a critical regulator of HIV-1 infection in human CD4 T cells and thymocytes.

Regulation of Glut1, the major glucose transporter in T lymphocytes, is quite complex, as it is controlled at the level of transcription, translation, and transport to the cell surface. Indeed, in most cell types, it is glucose uptake across the plasma membrane that is the rate-limiting step in the production of ATP. In response to low $O_2$ levels, the enhanced expression and function of Glut1 is mediated, at least in part, by the hypoxia-inducible factor 1 transcription factor (31). Augmented Glut1 levels have been shown to play an important role in the survival and "fitness" of tumor cells adapted to hypoxic conditions (reviewed in ref. 45) but, to our knowledge, this is a unique report showing that Glut1 levels on T cells can be modulated by the $O_2$ conditions to which they are exposed.

Surface Glut1 levels on CD4 T cells were augmented at 2.5% $O_2$ levels following IL-7 stimulations (Fig. 3). The high repercussion on glucose uptake, with a dramatic 300% increase in

transport, is likely due not only to increased Glut expression but also to conformational changes in Glut1 itself. It has been shown that cytoplasmic ATP inhibits Glut1-mediated glucose uptake by favoring an interaction between the Glut1 C terminus and Glut1 cytoplasmic loop 6–7 (46). Therefore, under conditions where ATP levels are lower at physiological $O_2$ concentrations compared with atmospheric $O_2$, the Glut1 conformation would be, at least, partially released from this inhibitory effect.

It is well-known that efficient HIV-1 infection is highly dependent on T-cell activation and cell cycle entry, with quiescent lymphocytes showing very inefficient HIV-1 infection (reviewed in ref. 5). This paradoxical observation, in the context of a lentivirus otherwise shown to infect nondividing cells, has been puzzling. The factor(s) controlling infection in resting T cells has not yet been completely elucidated, but recent studies indicate important roles for cellular c-Jun N-terminal kinase (47) and chemokine-induced changes in the actin cytoskeleton (48). The role of the PI3K pathway in HIV infection of primary T cells is somewhat controversial, as early studies, performed in transformed cell lines and activated T cells, reported that PI3K negatively impacts HIV-1 transcription (48), whereas later work found that PI3K signaling is required for HIV integration in chemokine-treated quiescent CD4^{+} T cells (49). The results reported here are in agreement with the more recent study, as blocking PI3K signaling in IL-7–stimulated resting T cells abrogated HIV-1 infection. Furthermore, our data suggest that inhibition of HIV-1 infection by PI3K inhibitors is mediated, at least in part, via the suppression of Glut1 expression and function.

Our finding that IL-7–mediated glucose uptake is associated with a sustained permissivity to HIV-1 infection at physiological $O_2$ levels brings unique perspectives to previous reports showing that G0-phase T cells can be infected by HIV-1 when present in lymphoid aggregate cultures (1, 2, 50). Specifically, in these latter conditions, aimed at more faithfully reproducing the in vivo system, T cells within the aggregates would be exposed to significantly lower levels of $O_2$ than those delivered to suspension T cells cultured under atmospheric conditions. Although we reveal the Glut1-mediated pathway as critically impacting on HIV-1 infection under both atmospheric and physiological $O_2$ concentrations, it is likely that $O_2$ modulates IL-7–mediated HIV-1 infection via other pathways as well. Intriguingly, the transactivational properties of the HIV-1 Tat protein promote HIV-1 infection at physiological but not atmospheric $O_2$ conditions (51). Thus, it will be of interest to reassess some of the earlier ex vivo HIV studies to determine whether the data were modulated by the $O_2$ tensions at which the experiments were performed.

The ensemble of the data presented here strongly suggests a role for IL-7 in reversing HIV-1 latency in the low $O_2$ environments found in spleen, lymph nodes, and thymus, thereby eliminating latent reservoirs (reviewed in ref. 8). It will be important to assess whether IL-7 administration modulates glucose uptake and metabolism in T lymphocytes of HIV-1–infected patients and to determine whether the outcome of IL-7 cytokine therapy differs in the high $O_2$ environment of the peripheral circulation compared with the relatively low $O_2$ state of lymphoid organs.

## Materials and Methods

**Cell Isolation and Culture.** T cells were isolated from adult peripheral blood, umbilical cord blood, and thymi as described in *SI Materials and Methods*. Cells were cultured in RPMI media supplemented with human recombinant IL-7 (10 ng/mL; kindly provided by Cytheris) as described in *SI Materials and Methods* and, when indicated, LY294002 was added.

**Flow Cytometry.** To detect expression of surface markers, cells were incubated with the appropriate fluorochrome-conjugated mAbs (BD Biosciences), or with 7-amino-actinomycin-D and pyronin Y as described in *SI Materials and Methods*. Surface Glut1 expression was monitored by binding to a recombinant human T-lymphotrophic virus-2 envelope receptor-binding domain (HRBD) fused to the EGFP coding sequence (HRBDEGFP) as described (41, 52).

**Glucose Uptake Assays.** Uptake was performed for 10 min at room temperature upon addition of 2-deoxy-D-[1-³H]glucose (Amersham Biosciences) as described in *SI Materials and Methods*.

**siRNA Transfections for Glut1 Inhibition and Analyses of Glut1 Transcripts.** Purified T cells were transfected with the indicated synthetic siRNAs, complementary to the Glut1 3′ UTR (41), as described in *SI Materials and Methods*. Quantitative PCR for Glut1 and 18S was performed as described in *SI Materials and Methods*.

**Virus Production and Infections.** Self-inactivating single-round HIV-1 virions were generated by transient transfection of 293T cells as published (53) and described in *SI Materials and Methods*. For single-round infections, lymphocytes were infected with HIVenv712-pseudotyped vector or VSV-G–pseudotyped HIV-1 vector as indicated in *SI Materials and Methods*.

1. Eckstein DA, et al. (2001) HIV-1 actively replicates in naive CD4⁺ T cells residing within human lymphoid tissues. *Immunity* 15:671–682.
2. Kinter A, Moorthy A, Jackson R, Fauci AS (2003) Productive HIV infection of resting CD4⁺ T cells: Role of lymphoid tissue microenvironment and effect of immunomodulating agents. *AIDS Res Hum Retroviruses* 19:847–856.
3. Korin YD, Zack JA (1998) Progression to the G1b phase of the cell cycle is required for completion of human immunodeficiency virus type 1 reverse transcription in T cells. *J Virol* 72:3161–3168.
4. Biancotto A, et al. (2008) HIV-1 induced activation of CD4⁺ T cells creates new targets for HIV-1 infection in human lymphoid tissue ex vivo. *Blood* 111:699–704.
5. Vatakis DN, Nixon CC, Zack JA (2010) Quiescent T cells and HIV: An unresolved relationship. *Immunol Res* 48(1–3):110–121.
6. Brooks DG, et al. (2003) Molecular characterization, reactivation, and depletion of latent HIV. *Immunity* 19:413–423.
7. Chomont N, et al. (2009) HIV reservoir size and persistence are driven by T cell survival and homeostatic proliferation. *Nat Med* 15:893–900.
8. Lewin SR, Rouzioux C (2011) HIV cure and eradication: How will we get from the laboratory to effective clinical trials? *AIDS* 25:885–897.
9. Kim GY, Hong C, Park JH (2011) Seeing is believing: Illuminating the source of in vivo interleukin-7. *Immune Netw* 11(1):1–10.
10. Fry TJ, Mackall CL (2005) The many faces of IL-7: From lymphopoiesis to peripheral T cell maintenance. *J Immunol* 174:6571–6576.
11. Rosenberg SA, et al. (2006) IL-7 administration to humans leads to expansion of CD8⁺ and CD4⁺ cells but a relative decrease of CD4⁺ T-regulatory cells. *J Immunother* 29: 313–319.
12. Sportès C, et al. (2008) Administration of rhIL-7 in humans increases in vivo TCR repertoire diversity by preferential expansion of naive T cell subsets. *J Exp Med* 205: 1701–1714.
13. Sportès C, et al. (2010) Phase I study of recombinant human interleukin-7 administration in subjects with refractory malignancy. *Clin Cancer Res* 16:727–735.
14. Levy Y, et al. (2009) Enhanced T cell recovery in HIV-1-infected adults through IL-7 treatment. *J Clin Invest* 119:997–1007.
15. Sereti I, et al.; ACTG 5214 Study Team (2009) IL-7 administration drives T cell-cycle entry and expansion in HIV-1 infection. *Blood* 113:6304–6314.
16. Caldwell CC, et al. (2001) Differential effects of physiologically relevant hypoxic conditions on T lymphocyte development and effector functions. *J Immunol* 167: 6140–6149.
17. Westermann J, Pabst R (1992) Distribution of lymphocyte subsets and natural killer cells in the human body. *Clin Investig* 70:539–544.
18. Sopper S, et al. (2003) Impact of simian immunodeficiency virus (SIV) infection on lymphocyte numbers and T-cell turnover in different organs of rhesus monkeys. *Blood* 101:1213–1219.
19. Robbins JR, et al. (2005) Hypoxia modulates early events in T cell receptor-mediated activation in human T lymphocytes via Kv1.3 channels. *J Physiol* 564(Pt 1):131–143.
20. Atkuri KR, Herzenberg LA, Niemi AK, Cowan T, Herzenberg LA (2007) Importance of culturing primary lymphocytes at physiological oxygen levels. *Proc Natl Acad Sci USA* 104:4547–4552.
21. Larbi A, Zelba H, Goldeck D, Pawelec G (2010) Induction of HIF-1α and the glycolytic pathway alters apoptosis and differentiation profiles of activated human T cells. *J Leukoc Biol* 87:265–273.
22. Makino Y, et al. (2003) Hypoxia-inducible factor regulates survival of antigen receptor-driven T cells. *J Immunol* 171:6534–6540.
23. Roman J, et al. (2010) T-cell activation under hypoxic conditions enhances IFN-γ secretion. *Am J Respir Cell Mol Biol* 42(1):123–128.
24. Park JH, et al. (2004) Suppression of IL7Rα transcription by IL-7 and other prosurvival cytokines: A novel mechanism for maximizing IL-7-dependent T cell survival. *Immunity* 21:289–302.
25. Swainson L, Verhoeyen E, Cosset FL, Taylor N (2006) IL-7R α gene expression is inversely correlated with cell cycle progression in IL-7-stimulated T lymphocytes. *J Immunol* 176:6702–6708.
26. Alves NL, van Leeuwen EM, Derks IA, van Lier RA (2008) Differential regulation of human IL-7 receptor α expression by IL-7 and TCR signaling. *J Immunol* 180: 5201–5210.
27. Jourdan P, et al. (1998) IL-4 induces functional cell-surface expression of CXCR4 on human T cells. *J Immunol* 160:4153–4157.
28. Soares MV, et al. (1998) IL-7-dependent extrathymic expansion of CD45RA⁺ T cells enables preservation of a naive repertoire. *J Immunol* 161:5909–5917.
29. Hassan J, Reen DJ (2001) Human recent thymic emigrants—Identification, expansion, and survival characteristics. *J Immunol* 167:1970–1976.
30. Dardalhon V, et al. (2001) IL-7 differentially regulates cell cycle progression and HIV-1-based vector infection in neonatal and adult CD4⁺ T cells. *Proc Natl Acad Sci USA* 98: 9277–9282.
31. Bashan N, Burdett E, Hundal HS, Klip A (1992) Regulation of glucose transport and GLUT1 glucose transporter expression by O₂ in muscle cells in culture. *Am J Physiol* 262:C682–C690.
32. Rathmell JC, Elstrom RL, Cinalli RM, Thompson CB (2003) Activated Akt promotes increased resting T cell size, CD28-independent T cell growth, and development of autoimmunity and lymphoma. *Eur J Immunol* 33:2223–2232.
33. Frauwirth KA, et al. (2002) The CD28 signaling pathway regulates glucose metabolism. *Immunity* 16:769–777.
34. Manel N, et al. (2003) The HTLV receptor is an early T-cell activation marker whose expression requires de novo protein synthesis. *Blood* 101:1913–1918.
35. Chakrabarti R, Jung CY, Lee TP, Liu H, Mookerjee BK (1994) Changes in glucose transport and transporter isoforms during the activation of human peripheral blood lymphocytes by phytohemagglutinin. *J Immunol* 152:2660–2668.
36. Kinet S, et al. (2007) Isolated receptor binding domains of HTLV-1 and HTLV-2 envelopes bind Glut-1 on activated CD4⁺ and CD8⁺ T cells. *Retrovirology* 4:31.
37. Yu Q, Erman B, Bhandoola A, Sharrow SO, Singer A (2003) In vitro evidence that cytokine receptor signals are required for differentiation of double positive thymocytes into functionally mature CD8⁺ T cells. *J Exp Med* 197:475–487.
38. Barata JT, et al. (2004) Activation of PI3K is indispensable for interleukin 7-mediated viability, proliferation, glucose use, and growth of T cell acute lymphoblastic leukemia cells. *J Exp Med* 200:659–669.
39. Maciver NJ, et al. (2008) Glucose metabolism in lymphocytes is a regulated process with significant effects on immune cell function and survival. *J Leukoc Biol* 84: 949–957.
40. Montel-Hagen A, Sitbon M, Taylor N (2009) Erythroid glucose transporters. *Curr Opin Hematol* 16(3):165–172.
41. Montel-Hagen A, et al. (2008) Erythrocyte Glut1 triggers dehydroascorbic acid uptake in mammals unable to synthesize vitamin C. *Cell* 132:1039–1048.
42. Rosenzweig M, Clark DP, Gaulton GN (1993) Selective thymocyte depletion in neonatal HIV-1 thymic infection. *AIDS* 7:1601–1605.
43. Kitchen SG, Zack JA (1997) CXCR4 expression during lymphopoiesis: Implications for human immunodeficiency virus type 1 infection of the thymus. *J Virol* 71:6928–6934.
44. Swainson L, et al. (2005) Glucose transporter 1 expression identifies a population of cycling CD4⁺ CD8⁺ human thymocytes with high CXCR4-induced chemotaxis. *Proc Natl Acad Sci USA* 102:12867–12872.
45. Macheda ML, Rogers S, Best JD (2005) Molecular and cellular regulation of glucose transporter (GLUT) proteins in cancer. *J Cell Physiol* 202:654–662.
46. Blodgett DM, De Zutter JK, Levine KB, Karim P, Carruthers A (2007) Structural basis of GLUT1 inhibition by cytoplasmic ATP. *J Gen Physiol* 130(2):157–168.
47. Manganaro L, et al. (2010) Concerted action of cellular JNK and Pin1 restricts HIV-1 genome integration to activated CD4⁺ T lymphocytes. *Nat Med* 16:329–333.
48. Saleh S, et al. (2011) Expression and reactivation of HIV in a chemokine induced model of HIV latency in primary resting CD4⁺ T cells. *Retrovirology* 8:80.
49. Saleh S, Cameron P, Sallmann G, Joworowski A, Lewin SR (2011) The PI3K signaling pathway is critical for HIV integration in latently infected resting CD4⁺ T cells. *Sixth IAS Conference on HIV Pathogenesis, Treatment and Prevention*. Available at http://pag.ias2011.org/abstracts.aspx?aid=2243.
50. Zhang Z, et al. (1999) Sexual transmission and propagation of SIV and HIV in resting and activated CD4⁺ T cells. *Science* 286:1353–1357.
51. Sahaf B, et al. (2008) Culturing of human peripheral blood cells reveals unsuspected lymphocyte responses relevant to HIV disease. *Proc Natl Acad Sci USA* 105:5111–5116.
52. Manel N, et al. (2003) The ubiquitous glucose transporter GLUT-1 is a receptor for HTLV. *Cell* 115:449–459.
53. Verhoeyen E, et al. (2003) IL-7 surface-engineered lentiviral vectors promote survival and efficient gene transfer in resting primary T lymphocytes. *Blood* 101:2167–2174.

# Supporting Information

## Loisel-Meyer et al. 10.1073/pnas.1121427109

### SI Materials and Methods

**Cell Isolation and Culture.** Adult peripheral blood (APB), obtained from healthy donors after informed consent, was collected in heparin-containing tubes. Umbilical cord blood (UCB) was obtained after informed consent, immediately after delivery of full-term infants. Thymi were removed during corrective cardiac surgery of patients in accordance with local ethics board regulations. CD4 T cells or total CD3 T cells were purified using negative-selection Rosette tetramers (StemCell Technologies). To subsequently isolate naive and memory T cell subsets by negative selection, CD4 lymphocytes were incubated with αCD45RO (Dako) or αCD45RA (Immunotech) mAbs, respectively, in combination with αHLA-DR and αCD69 mAbs, to eliminate preactivated T cells. The non-bound fractions were recovered following addition of α-mouse IgG-conjugated magnetic beads (Dynal). The purity of each cell population was monitored on a FACSCalibur (BD Pharmingen).

**Cell Culture Conditions.** Lymphocytes were cultured in RPMI medium 1640 (Gibco-BRL Invitrogen) supplemented with 10% (vol/vol) FCS, herein referred to as R10 medium. For IL-7 stimulation, human recombinant IL-7 (10 ng/mL; kindly provided by Cytheris) was replenished every 2–3 days. Cells were maintained in either a standard tissue culture incubator containing atmospheric (20%) $O_2$ or an incubator where 2.0–2.5% $O_2$ conditions were maintained by nitrogen injections (Heraeus incubator; Sanyo) and $CO_2$ was maintained at 5%. In indicated experiments, LY294002 (Sigma) was added to cultures at 15 µM 1 h before IL-7 stimulation.

**Flow Cytometry.** To detect expression of surface markers, cells were incubated with the appropriate fluorochrome-conjugated mAbs (BD Biosciences) and monitored compared with an Ig isotype antibody. The tyrosine phosphorylation state of STAT5 was assessed using an anti–phospho-STAT5 (Y694) antibody (BD Pharmingen). Cell cycle analysis was performed by DNA and RNA stains using 7-amino-actinomycin-D (7AAD; 20 µM; Sigma) and pyronin Y (PY; 5 µM; Sigma), respectively, or with an αKi67 mAb (Dako). Cells were analyzed on a FACSCalibur or FACS-Canto (BD Biosciences) using BD Biosciences or FlowJo software (Tree Star).

**Glucose Uptake Assays.** Cells ($2 \times 10^6$) were starved by incubation at 37 °C in serum/glucose-free RPMI for 30 min. Radiolabeled 2-deoxy-D-[1-$^3$H]glucose (Amersham Biosciences) was added to a final concentration of 0.1 mM (2 µCi/mL). Cells were incubated for 10 min at room temperature, washed in cold serum/glucose-free RPMI, and solubilized in 500 µL 0.1% SDS. Radioactivity was measured by liquid scintillation.

**siRNA Transfections for Glut1 Inhibition.** Purified T cells were transfected with the indicated synthetic siRNAs, complementary to the Glut1 3′ UTR (1), using the Human T Cell Nucleofector Kit (Amaxa) per the manufacturer's protocol.

Sequences of siRNAs for Glut1 inhibition: 5′-UGAUGUCC-AGAAGAAUAUU-3′; 5′-UAUUAAAUACAGACACUAA-3′; 5′-AGCUUCUAUCCCAGGAGGU-3′. Sequence of control siRNAs (luciferase): 5′-CUUACGCUGAGUACUUCGA-3′.

**Quantitative Analysis of Glut1 Transcripts.** Total RNA was isolated using an RNeasy Kit (Qiagen). Quantitative PCR of cDNAs was performed using Quantitect SYBR Green PCR Master Mix (Roche). Primers were designed within a single exon, allowing the efficacy of primer pairs to be verified on genomic DNA samples, and standard curves for amplification products were established on genomic DNA. Amplification of cDNAs was performed using a LightCycler 480 (Roche). Cycling conditions comprised a denaturation step for 5 min at 95 °C, followed by 40 cycles of denaturation (95 °C for 10 s), annealing (63 °C for 10 s), and extension (72 °C for 10 s). After amplification, melting curve analysis was performed with denaturation at 95 °C for 5 s and continuous fluorescence measurement from 65 °C to 97 °C at 0.1 °C/s. Each sample was amplified in duplicate. Relative expression was calculated by normalization to 18S RNA.

Quantitative RT-PCR primers for Glut1: 5′-TGCTGATGATG-AACCTGCTG-3′ (forward); 5′-GATGAGGATGCCGACGAC-3′ (reverse). Quantitative RT-PCR primers for 18S: 5′-CGGCTAC-CACATCCAAGGAA-3′ (forward); 5′-GGGCCTCGAAAGAGT-CCTGT-3′ (reverse).

**Virus Production and Infection.** Self-inactivating single-round HIV-1 virions were generated by transient transfection of 293T cells with the GFP-encoding HIV-1 SIN vector pHIVSFFVGFP together with the Gag-Pol packaging construct 8.91. (2) For X4-HIV-1 envelope pseudotyping, 7 µg of HIVenv712 was cotransfected, whereas for VSV-G pseudotyping, 3 µg of pCMV-VSV-G plasmid was cotransfected. Viral supernatant was harvested 48 h post-transfection and concentrated by ultracentrifugation for 2 h at 4 °C at 25,000 rpm. To determine the HIV titers, serial dilutions of vector preparations were added to 293T cells or Jurkat cells (CD4$^+$CXCR4$^+$) for VSV-G and HIVenv712 pseudotypes, respectively. The titers are expressed as 293T or Jurkat (CD4$^+$CXCR4$^+$) transducing units (TU)/mL.

For single-round infections of CD4 T cells, viral supernatant containing $1 \times 10^6$ TU of HIVenv712-pseudotyped vector [multiplicity of infection (MOI) of 10] or 2–3 $\times 10^6$ TU of VSV-G–pseudotyped HIV-1 vector (MOI of 20–30) was added to $1 \times 10^5$ lymphocytes. After overnight infection, cells were washed and reseeded in 1 mL of IL-7–supplemented R10 media for 48 h. Infection was determined as the percentage of GFP$^+$ cells by flow cytometry.

**Statistics.** Statistical analyses were performed using a paired, two-tailed Student's $t$ test.

1. Montel-Hagen A, et al. (2008) Erythrocyte Glut1 triggers dehydroascorbic acid uptake in mammals unable to synthesize vitamin C. *Cell* 132:1039–1048.

2. Naldini L, et al. (1996) In vivo gene delivery and stable transduction of nondividing cells by a lentiviral vector. *Science* 272(5259):263–267.
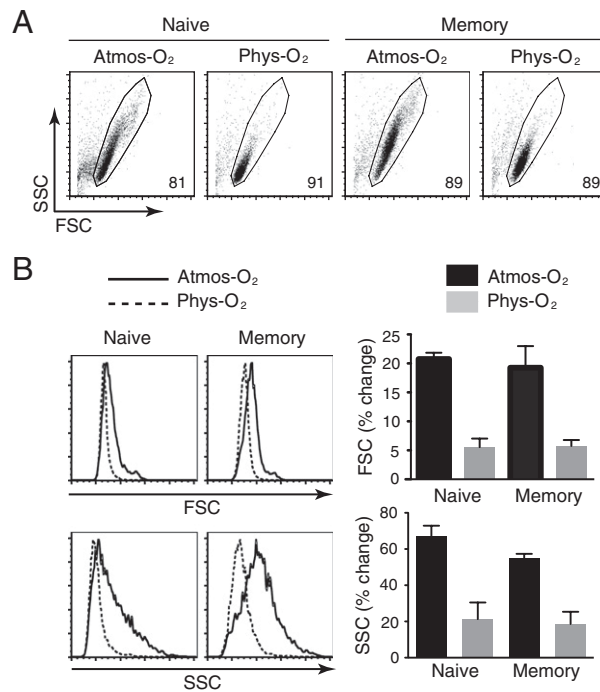
**Fig. S1.** IL-7 promotes CD4 T-cell survival at both atmospheric and physiological oxygen concentrations. Naive and memory CD4 T cell populations isolated from APB were stimulated with IL-7 (10 ng/mL) under 20% (Atmos-$O_2$) or 2.5% (Phys-$O_2$) $O_2$ conditions. (A) Cell size and granularity were assessed as a measure of forward scatter (FSC) and side scatter (SSC), respectively. The percentages of cells within the live gate are indicated. (B) Overlays of histograms showing the FSC and SSC profiles of CD4 T cells after 9 days of IL-7 stimulation at Atmos-$O_2$ (continuous line) and Phys-$O_2$ (dotted line) are shown (*Left*). Quantifications of the mean percentage changes in mean fluorescence intensity (MFI) relative to day 0 nonstimulated controls ± SD are shown (*Right*).
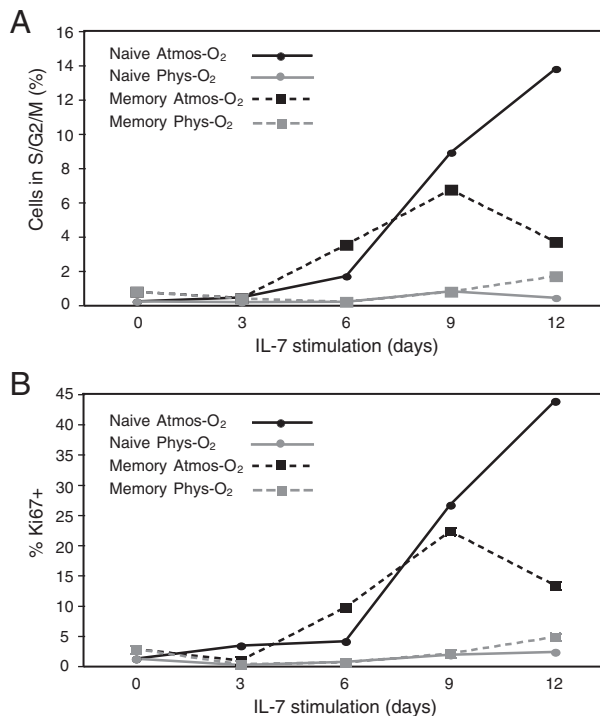


**Fig. S2.** Kinetics of cell cycle progression of IL-7–stimulated naive and memory CD4 T cells. Naive and memory APB CD4 T cell populations were stimulated with IL-7 (10 ng/mL) under 20% (Atmos-$O_2$) or 2.5% (Phys-$O_2$) oxygen conditions. Cell cycle progression was monitored at days 3, 6, 9, and 12 of culture under Atmos-$O_2$ and Phys-$O_2$ conditions, as a function of PY/7AAD (A) and Ki67 (B) staining. Data are representative of at least three independent experiments comprising three to four different donors.
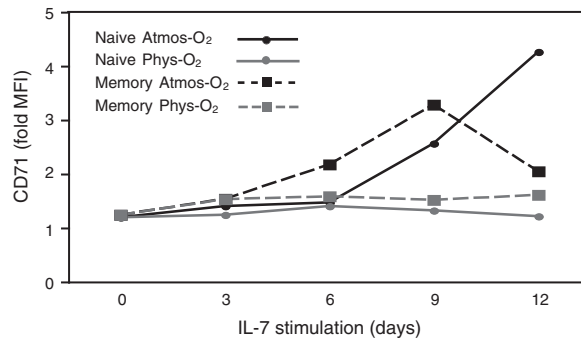
**Fig. S3.** Kinetics of IL-7–induced CD71 up-regulation at physiological and atmospheric oxygen concentrations. Naive and memory APB CD4 T cells remained unstimulated or were stimulated with IL-7 (10 ng/mL) under 20% (Atmos-$O_2$) or 2.5% (Phys-$O_2$) oxygen conditions. Quantification of the relative levels of CD71, monitored as a function of the fold change in ΔMFI, is presented for days 0, 3, 6, 9, and 12 of IL-7 stimulation. Data are representative of three independent experiments comprising four different donors.
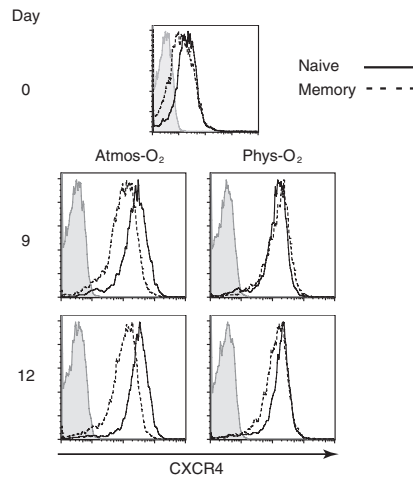


**Fig. S4.** IL-7–induced CXCR4 expression is maintained at 2–20% oxygen concentrations. CXCR4 expression was monitored on naive and memory APB CD4 T cell populations following IL-7 stimulation. Histograms show CXCR4 staining (open histograms) compared with isotype controls (closed histograms) at 0, 9, and 12 days of IL-7 stimulation at 20% (Atmos-$O_2$) and 2.5% (Phys-$O_2$) oxygen conditions. Data are representative of three independent experiments comprising eight different donors.
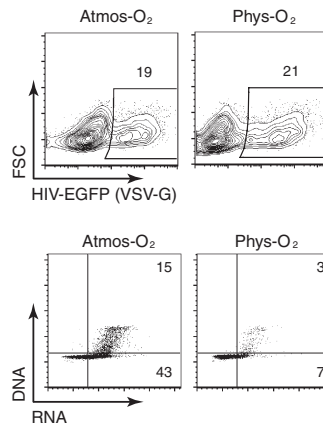


**Fig. S5.** Permissivity of cord blood T cells to single-round infection with VSV-G–pseudotyped HIV-1 virions is independent of cell cycle entry under physiological oxygen conditions. UCB CD4 T cells were stimulated with IL-7 for 4 days and then infected with VSV-G envelope-pseudotyped HIV-1 virions expressing EGFP. Cell cycle entry was assessed at the time of infection by PY/7AAD staining, and the percentages of cells in the G1b (lower right quadrant) and S/G2/M (upper right quadrant) phases of the cell cycle are indicated (*Lower*). The percentages of HIV-EGFP+ cells are indicated. Data are representative of five independent experiments comprising five different donors.
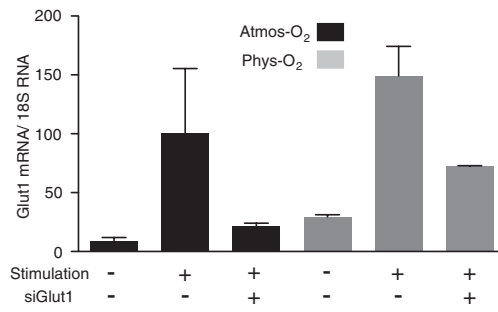
**Fig. S6.** Inhibition of Glut1 transcription by Glut1-specific siRNAs. CD4 T cells from APB were transfected with Glut1-specific siRNAs (siGlut1) and then stimulated under 20% (Atmos-$O_2$) or 2.5% (Phys-$O_2$) conditions for 24 h. Glut1 transcripts were quantified by quantitative RT-PCR; cDNAs were amplified with Glut1-specific primers and normalized to 18S transcripts. The means $\pm$ SD for triplicate samples are shown.